

Photoluminescence efficiency of zincblende InGaN/GaN quantum wells

S. A. Church,¹ M. Quinn,¹ K. Cooley-Greene,¹ B. Ding,² A. Gundimeda,² M. J. Kappers,² M. Frentrup,² D. J. Wallis,^{2,3} R. A. Oliver,² and D. J. Binks¹

¹*Department of Physics and Astronomy, Photon Science Institute, University of Manchester, Manchester M13 9PL, United Kingdom*

²*Department of Materials Science and Metallurgy, University of Cambridge, 27 Charles Babbage Road, Cambridge CB3 0FS, United Kingdom*

³*Centre for High Frequency Engineering, University of Cardiff, 5 The Parade, Newport Road, Cardiff, CF24 3AA, United Kingdom*

S1. SUPPLEMENTARY MATERIAL

Fig S1 shows an STEM HAADF image of the SQW sample, in which significant buckling is evident. Previous work has shown that this buckling is produced when stacking faults intersect the QW¹.

Polarisation-resolved photoluminescence (PL) spectra were measured for the five-QW samples at 10 K by placing a Glan-Thompson polariser in front of the collection slit of the spectrometer, and the results are shown in Fig. S2. The response of the spectrometer was corrected for in each polarisation direction. The samples all show a strong degree of linear polarisation (DOLP) in the [1-10] direction, which is approximately uniform across the spectrum. The spectrally integrated DOLP is given in Fig. S3 for each sample, with values of 69 %, 57 % and 50 % for increasing QW width. These high values for the DOLP suggest that the emission originates from carrier recombination in Qwires embedded in the QWs^{1,2}.

As the Qwires are constrained in one-dimension by the QW itself, increasing the QW width will increase the cross sectional area of the Qwires. For Qwires of these sizes the DOLP depends strongly upon the cross sectional area³, and so increasing the QW width will result in a drop in the DOLP. This is consistent with Fig. S3

Previous studies on zb-InGaN/GaN QWs had an unpolarised peak which was attributed to recombination in the QWs away from the Qwires². This unpolarised peak is not visible in the spectra in Fig S2, suggesting that carrier capture into the Qwires is more efficient for these samples compared with those studied previously. A weak second peak is just visible at an energy of 2.4 eV

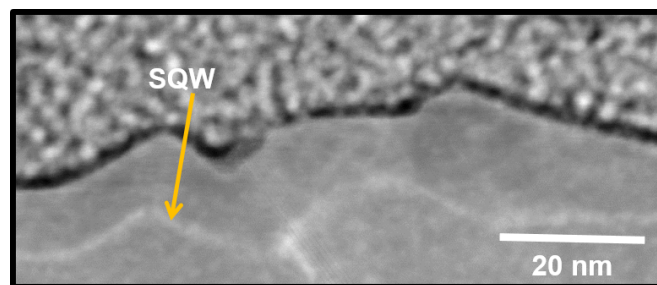


FIG. S1. STEM HAADF image of the SQW region showing the buckling caused by stacking faults.

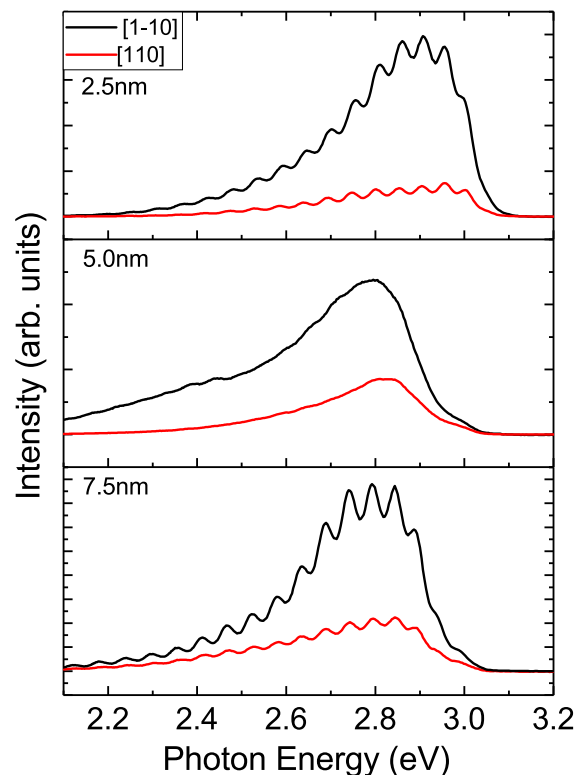


FIG. S2. 10 K polarised PL spectra for the zb-InGaN/GaN five-QWs with different QW widths at an excitation power density of 10 W/cm².

for the 5.0 nm QW sample. However, since this peak is polarised, the distribution of Qwires in this sample may be bi-modal.

To understand how the low temperature PL peak energy varies with QW width and In content, the ground state electron-hole transition energies of the Qwires were calculated. Carriers in the Qwire were treated as being confined in a finite square potential well that is 2 nm in size in one direction, corresponding to the width of In segregation region adjacent to a stacking fault, and of a size equal to the QW width in an orthogonal direction. For the confinement due to the In segregation, the potential barrier was found from the difference in band gap

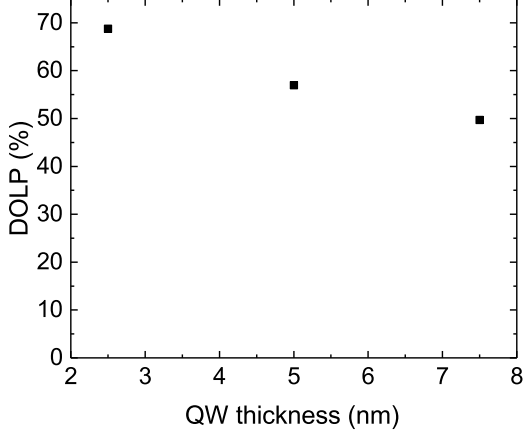


FIG. S3. The 10K DOLP of the emission from zb-InGaN/GaN QWs calculated from the integrated intensity of the PL spectra in Fig. S1.

between the QW and Qwire; for confinement by the limits of the QW, the potential corresponded to the band gap difference between the Qwire and the GaN barrier. In both cases the valance band offset was assumed to be 20%. The InGaN bandgaps in the QW and Qwire were calculated using Vegard's Law with a bowing parameter of 1.4⁴; the In content in the Qwire was taken as being 2.3 times greater than in the QW, due to the In segregation effect reported previously^{1,2}. Similarly, the effective masses for both electrons and holes in the QW and Qwire were calculated from the values for GaN and InN using Vegard's Law. All the parameter values used are given in Table S1. The energy, E , due to the confinement of a carrier of effective mass, m , by a square of potential well of width, L , and height, V , was determined by numerically finding the lowest energy solution to [4]:

$$\alpha = k \tan\left(\frac{kL}{2}\right) \quad (1)$$

where

$$\alpha = \sqrt{\frac{2m(V-E)}{\hbar}} \quad (2)$$

and

$$k = \sqrt{\frac{2mE}{\hbar}} \quad (3)$$

The total confinement energy is the sum of four contributions: the energies due to confinement in each of the two directions and for each of the two carriers. The recombination energy was found by adding the total confinement energy to the bandgap of the Qwire and then subtracting an exciton binding energy of 26 meV⁵.

Fig S4 shows the variation of the calculated recombination energy for QW widths from 2 nm to 8 nm and for

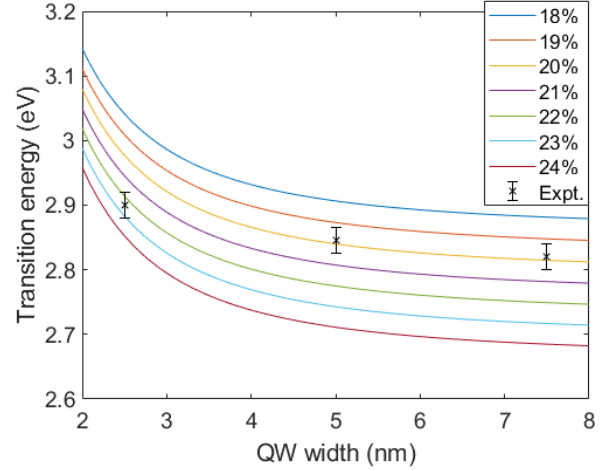


FIG. S4. The 10K experimental PL peak energies for the three QW widths studied compared to the recombination energies calculated for quantum wires with In fractions of 18%, 19%, 20%, 21%, 22%, 23% and 24%. The quantum wires are 2nm wide in one direction and as wide as the QW in an orthogonal direction.

	E_g (eV)	m_h^* (m_0)	m_e^* (m_0)
GaN	3.30 ⁶	0.61 ⁶	0.19 ⁶
InN	0.596 ⁷	0.5 ⁷	0.041 ⁸

TABLE S1. Parameters used for calculating the ground state transition energies.

QWire In contents from 18% to 24%, corresponding to In contents in the QW from 7.8% to 10.4%. The dependence of the recombination energy on QW width is seen to be significant for widths less than about 5 nm, but becomes weak for larger QW sizes. In contrast, increasing the In content redshifts the recombination energy significantly for all QW sizes. Thus, for QW sizes larger than approximately 5 nm, the recombination energy will depend principally on In content so that QW width can be varied without restricting the emission energies achievable. Also, plotted in Fig S4 are the peak energies for the samples studied experimentally. The peak energies for the 5 nm and 7.5 nm QW widths agree well with the calculations for 20% In content in the QWire (corresponding to 9% in the QW). In contrast, the peak energy for the 2.5 nm QW width is in better agreement with an In content of 22% (corresponding to 10% in the QW). However, a constant exciton binding energy is used in these calculations with the value corresponding to bulk zb-GaN. As noted in the main manuscript, the reduction of the recombination lifetime from 680 ps to 530 ps as QW width is reduced is consistent with an increase in binding energy, suggesting that it has been underestimated, particularly for the 2.5 nm QW width sample. This may explain the apparent deviation of the thinnest QW sam-

ple from the same In content as the other samples. The uncertainty in the In content of the QWires ($\pm 0.5\%$) is derived from the errors on the experimental peak energies, as shown in Fig S4. However, the uncertainty in the In content of the QWs ($\pm 5\%$) is dominated by the contribution from the In content ratio between Qwires and QWs, which has been determined previously¹ to be 2.3 ± 1.2 .

¹B. Ding, M. Frentrup, S. M. Fairclough, M. J. Kappers, M. Jain, A. Kovács, D. J. Wallis, and R. A. Oliver, *J. Appl. Phys.* **128**, 145703 (2020).

²S. A. Church, B. Ding, P. W. Mitchell, M. J. Kappers, M. Fren-

trup, G. Kusch, S. M. Fairclough, D. J. Wallis, R. A. Oliver, and D. J. Binks, *Appl. Phys. Lett.* **117**, 032103 (2020).

³W. H. Zheng, J.-b. Xia, and K. W. Cheah, *J. Phys. Condens. Matter* **9**, 5105 (1997).

⁴J. Wu, W. Walukiewicz, K. M. Yu, J. W. Ager, E. E. Haller, H. Lu, and W. J. Schaff, *Appl. Phys. Lett.* **80**, 4741 (2002).

⁵D. J. As, F. Schmilgus, C. Wang, B. Schottker, D. Schikora, and K. Lischka, *Appl. Phys. Lett.* **70**, 1311 (1997).

⁶E. Baron, R. Goldhahn, M. Deppe, D. J. As, and M. Feneberg, *Phys. Rev. Mater.* **3**, 104603 (2019).

⁷H. Sanada, T. Sogawa, H. Gotoh, H. Kamada, H. Yamaguchi, and H. Nakano, *Phys Status Solidi C* **5**, 2904 (2008).

⁸P. Schley, R. Goldhahn, C. Napierala, G. Gobsch, J. Schörmann, D. J. As, K. Lischka, M. Feneberg, and K. Thonke, *Semicond. Sci. Technol.* **23**, 055001 (2008).